Inorganic Chemistry
Article

Inorg. Chem. **2010**, *49*, 8997–9004 **8997**
DOI: 10.1021/ic101275m

NMR Spectroscopic Evidence for the Intermediacy of XeF_3^- in XeF_2/F^- Exchange, Attempted Syntheses and Thermochemistry of XeF_3^- Salts, and Theoretical Studies of the XeF_3^- Anion

Neil Vasdev,[†,‡] Matthew D. Moran,[†] Heikki M. Tuononen,[§] Raman Chirakal,[†,‡] Reijo J. Suontamo,[§] Alex D. Bain,[†] and Gary J. Schrobilgen*[,†]

[†]*Department of Chemistry, McMaster University, Hamilton, Ontario L8S 4M1, Canada,* [‡]*Department of Nuclear Medicine, McMaster University Medical Centre and Hamilton Health Sciences, Hamilton, Ontario L8N 3Z5, Canada, and* [§]*Department of Chemistry, University of Jyväskylä, P.O. Box 35, FIN-40014, Jyväskylä, Finland*

Received June 26, 2010

The existence of the trifluoroxenate(II) anion, XeF_3^-, had been postulated in a prior NMR study of the exchange between fluoride ion and XeF_2 in CH_3CN solution. The enthalpy of activation for this exchange, $\Delta H^{\ddagger}$, has now been determined by use of single selective inversion ^{19}F NMR spectroscopy to be 74.1 ± 5.0 kJ mol^{-1} (0.18 M) and 56.9 ± 6.7 kJ mol^{-1} (0.36 M) for equimolar amounts of $[N(CH_3)_4][F]$ and XeF_2 in CH_3CN solvent. Although the XeF_3^- anion has been observed in the gas phase, attempts to prepare the Cs^+ and $N(CH_3)_4^+$ salts of XeF_3^- have been unsuccessful, and are attributed to the low fluoride ion affinity of XeF_2 and fluoride ion solvation in CH_3CN solution. The XeF_3^- anion would represent the first example of an AX_3E_3 valence shell electron pair repulsion (VSEPR) arrangement of electron lone pair and bond pair domains. Fluorine-19 exchange between XeF_2 and the F^- anion has also been probed computationally using coupled-cluster singles and doubles (CCSD) and density functional theory (DFT; PBE1PBE) methods. The energy-minimized geometry of the ground state shows that the F^- anion is only weakly coordinated to XeF_2 ($F_2Xe{-}{-}{-}F^-$; a distorted Y-shape possessing C_s symmetry), while the XeF_3^- anion exists as a first-order transition state in the fluoride ion exchange mechanism, and is planar and Y-shaped (C_{2v} symmetry). The molecular geometry and bonding of the XeF_3^- anion has been described and rationalized in terms of electron localization function (ELF) calculations, as well as the VSEPR model of molecular geometry. Quantum-chemical calculations, using the CCSD method and a continuum solvent model for CH_3CN, accurately reproduced the transition-state enthalpy observed by ^{19}F NMR spectroscopy, and showed a negative but negligible enthalpy for the formation of the $F_2Xe{-}{-}{-}F^-$ adduct in this medium.

Introduction

Of the binary xenon fluorides, only XeF_4 and XeF_6 are known to form anionic salts with fluoride ion donors. Xenon tetrafluoride behaves as a fluoride ion acceptor (calculated gas-phase fluoride ion affinity, FIA, 247.3 kJ mol^{-1})[1] toward alkali metal fluorides and the naked fluoride ion source $[N(CH_3)_4][F]$ to give salts of the pentagonal planar XeF_5^- anion.[2] Xenon hexafluoride is a considerably stronger fluoride ion acceptor (FIA, 313.8 kJ mol^{-1})[1] forming the XeF_7^- and XeF_8^{2-} anions with alkali metal (Na, K, Rb, Cs) fluorides.[3,4] In addition to the alkali metal fluoride salts, the NO^+ and NO_2^+ salts have been prepared by direct reaction of XeF_6 with NOF or NO_2F, namely, $[NO_2][XeF_7]$,[5] $[NO]_2[XeF_8]$,[6,7] and $[NO_2][Xe_2F_{13}]$.[5] Xenon hexafluoride also reacts with $[NF_4][HF_2]$ in anhydrous hydrogen fluoride (aHF) to give $[NF_4][XeF_7]$, which was converted to $[NF_4]_2[XeF_8]$ by selective laser photolysis and characterized by vibrational spectroscopy.[8] The $[NO]_2[XeF_8]$ salt was shown, by single-crystal X-ray diffraction, to contain the slightly distorted square antiprismatic XeF_8^{2-} anion.[6,7] The XeF_7^- and $Xe_2F_{13}^-$ anions have also been characterized by X-ray crystallography as their Cs^+ and NO_2^+ salts, respectively.[5] The XeF_7^- anion has a monocapped octahedral structure, while the $Xe_2F_{13}^-$ anion may be described as an XeF_6 molecule bridged by two long Xe−F bonds to an XeF_7^- anion such that the bridging fluorines avoid the nonbonding electron pair of the XeF_6 molecule.

In contrast, XeF_2 has not been conclusively shown by experiment to exhibit fluoride ion acceptor properties in solution or in

*To whom correspondence should be addressed. E-mail: schrobil@mcmaster.ca.

(1) Grant, D. J.; Wang, T.-H.; Dixon, D. A.; Christe, K. O. *Inorg. Chem.* **2010**, *49*, 261–270.
(2) Christe, K. O.; Curtis, E. C.; Dixon, D. A.; Mercier, H. P. A.; Sanders, J. C. P.; Schrobilgen, G. J. *J. Am. Chem. Soc.* **1991**, *113*, 3351–3361.
(3) Peacock, R. D.; Selig, H.; Sheft, I. *Proc. Chem. Soc.* **1964**, 285.
(4) Peacock, R. D.; Selig, H.; Sheft, I. *J. Inorg. Nucl. Chem.* **1966**, *28*, 2561–2567.
(5) Ellern, A.; Mahjoub, A.; Seppelt, K. *Angew. Chem., Int. Ed. Engl.* **1996**, *35*, 1123–1125.
(6) Peterson, S. W.; Holloway, J. H.; Coyle, B. A.; Williams, J. M. *Science* **1971**, *173*, 1238–1239.
(7) Adam, S.; Ellern, A.; Seppelt, K. *Chem.—Eur. J.* **1996**, *2*, 398–402.
(8) Christe, K. O.; Wilson, W. W. *Inorg. Chem.* **1982**, *21*, 4113–4117.

Published on Web 08/27/2010

the solid state (FIA, 83.3 kJ mol^{-1}).[1] The trifluoroxenate(II) anion, XeF_3^-, was first proposed to be a plausible anionic noble-gas species based on well-known diagonal trends within the Periodic Table.[9] The XeF_3^- anion was later proposed as an intermediate in the "base-catalyzed" fluorination of SO_2 by XeF_2;[10] however, reasonable alternative mechanisms were subsequently proposed for this reaction which did not involve the XeF_3^- anion.[11] Experimental evidence for the XeF_3^- anion has been obtained in the gas phase from the negative ion mass spectra of XeF_2[12] and $XeOF_4$,[13] and from energy-resolved collision-induced dissociation studies of XeF_2.[14] The related $XeF_3^•$ radical has recently been stabilized in an argon matrix and characterized by Fourier-transform infrared spectroscopy and explored by kinetic measurements.[15] The $XeF_3^•$ and $XeF_5^•$ radicals have been studied computationally and shown to be about 100 and 140 kcal mol^{-1} higher in energy than XeF_3^- and XeF_5^-, respectively, based on their heats of formation at 298 K.[1] Radiochemical experiments using ^{18}F (half-life = 109.7 min) have failed to confirm fluoride ion exchange with XeF_2 in water,[16] CH_2Cl_2,[17] or CH_3CN solvents.[17] However, $^{18}F^-$ exchanges between [^{18}F]-HF, [^{18}F]-SiF_4, and [^{18}F]-AsF_5 and XeF_2 have been successfully used for the preparation of [^{18}F]-XeF_2 (through XeF^+ and $Xe_2F_3^+$ as proposed intermediates),[18] which was, in turn, used for the preparation of [^{18}F]-2-fluoro-2-deoxy-D-glucose[19] and [^{18}F]-6-fluoro-L-3,4-dihydroxyphenylalanine.[20] Computational chemistry has more recently been employed to study the nature of the XeF_3^- anion in the gas phase,[1,14] as well as the thermodynamics of its formation (for details see Computational Results).[14]

In an earlier study, the authors observed exchange between F^- and XeF_2 in CH_3CN solvent under rigorously anhydrous conditions by use of 2-D $^{19}F-^{19}F$ EXSY experiments.[17] Fluorine-19 exchange occurred between the "naked" fluoride ion source, $[N(CH_3)_4][F]$, and XeF_2 in CH_3CN solvent at 15 °C, providing the first conclusive evidence for XeF_2/F^- exchange on the NMR time scale.[17] The ^{19}F exchange was postulated to proceed through the formation of XeF_3^- (eq 1).

$$XeF_2 + F^- \rightleftharpoons XeF_3^- \quad (1)$$

The objectives of the present study are to better define the nature of the XeF_2/F^- exchange, using single selective inversion NMR, and to establish the fluoride ion acceptor properties of XeF_2 by attempting the syntheses of representative salts containing the XeF_3^- anion. Computational methods (coupled-cluster singles and doubles (CCSD) and density functional theory (DFT)) have also been used to explore the nature of the XeF_2/F^- exchange. The current study also clarifies inconsistencies that have arisen in recent computational studies relating to the structure of the XeF_3^- anion.[1,14]

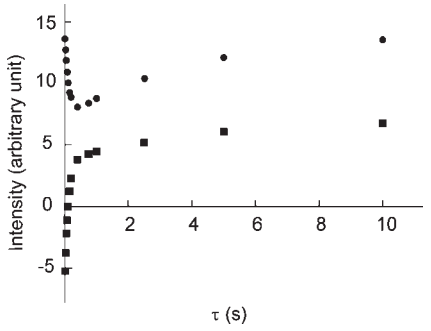

Figure 1. Enthalpy of activation, $\Delta H^‡$, determined by use of single selective inversion ^{19}F NMR spectroscopy to be 74.1 ± 5.0 kJ mol^{-1} from a stoichiometric sample (0.18 M in both $[N(CH_3)_4][F]$ and XeF_2 in CH_3CN solvent at −15 °C) of XeF_2 (●) and F^- (■).

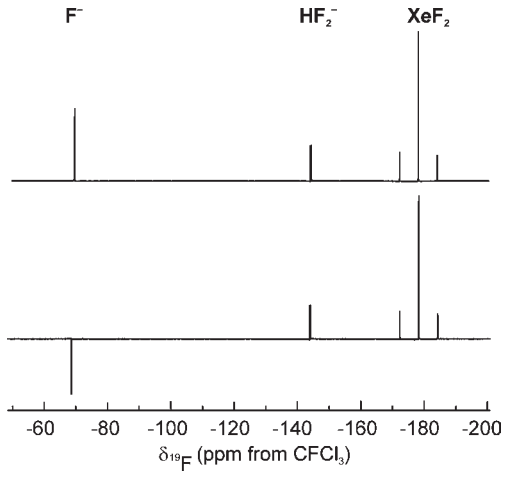

Figure 2. ^{19}F NMR resonances of XeF_2, $[N(CH_3)_4][F]$, and $[N(CH_3)_4][HF_2]$ in CH_3CN solvent (−15 °C). The 1-D NMR spectrum of XeF_2 and its natural abundance ^{129}Xe satellites and F^- (top trace) and the full-observed relaxation under the combined influence of spin−lattice relaxation and chemical exchange that results in the selective inversion of F^- with respect to XeF_2.

Results and Discussion

Intermolecular Exchange Between F^- and XeF_2. Although EXSY experiments are very effective for determining connectivities among exchanging sites, one-dimensional, single selective inversion experiments are considered to be superior for the study of slow exchange processes and for probing the thermodynamics of transition states.[21] The enthalpy of activation, $\Delta H^‡$, for intermolecular ^{19}F exchange between fluoride ion and XeF_2 was determined from two samples containing equimolar amounts of $[N(CH_3)_4][F]$ and XeF_2 in CH_3CN solvent (0.18 and 0.36 M), in conjunction with single selective inversion NMR spectroscopic experiments conducted at variable temperatures. Figure 1 shows the results of a ^{19}F selective inversion experiment acquired at −15 °C for a 0.18 M sample of XeF_2 and $[N(CH_3)_4][F]$ in CH_3CN solvent using various delay times. The analysis of this intermolecular exchange process was carried out over the temperature range −40 to 0 °C, and the data were fit, yielding a $\Delta H^‡$ value of 74.1 ± 5.0 kJ mol^{-1}. A more

(9) Ward, R. D. *J. Chem. Educ.* **1963**, *40*, 277–279.
(10) Wilson, I. L. *J. Fluorine Chem.* **1975**, *5*, 13–18.
(11) Liebman, J. F. *J. Fluorine Chem.* **1976**, *7*, 531–535.
(12) Begun, G. M.; Compton, R. N. *Int. J. Mass Spectrom. Ion Phys.* **1979**, *30*, 379–382.
(13) Studier, M. H.; Sloth, E. N. In *Noble Gas Compounds*; Hyman, H. H., Ed.; University of Chicago Press: Chicago, 1963; pp 47−49.
(14) Krouse, I. H.; Hao, C.; Check, C. E.; Lobring, K. C.; Sunderlin, L. S.; Wenthold, P. G. *J. Am. Chem. Soc.* **2007**, *129*, 846–852.
(15) Misochko, E. Y.; Akimov, A. V.; Belov, V. A.; Tyurin, D. A. *Inorg. Chem.* **2009**, *48*, 8723–8728.
(16) Appelman, E. H. *Inorg. Chem.* **1967**, *6*, 1268–1269.
(17) Vasdev, N.; Pointner, B. E.; Chirakal, R.; Schrobilgen, G. J. *J. Am. Chem. Soc.* **2002**, *124*, 12863–12868.
(18) Schrobilgen, G. J.; Firnau, G.; Chirakal, R.; Garnett, E. S. *J. Chem. Soc., Chem. Commun.* **1981**, 198–199.
(19) Sood, S.; Firnau, G.; Garnett, E. S. *Int. J. Appl. Radiat. Isot.* **1983**, *34*, 743–745.
(20) Firnau, G.; Chirakal, R.; Sood, S.; Garnett, E. S. *J. Labelled Compd. Radiopharm.* **1981**, *18*, 7–8.
(21) Bain, A. D.; Cramer, J. A. *J. Magn. Reson. A.* **1996**, *118*, 21–27.

concentrated sample (0.36 M XeF_2 and $[N(CH_3)_4][F]$ in CH_3CN solvent) was similarly analyzed over the temperature range −35 to −15 °C and yielded a $\Delta H^{\ddagger}$ value of 56.9 ± 6.7 kJ mol^{-1}. Because the two values are not statistically different (to within $\pm 3\sigma$) over the concentration and temperature ranges amenable for study by NMR spectroscopy, the values can be averaged (65.5 ± 8.4 kJ mol^{-1}) and are indicative of a single transition state (see Computational Results). The presence of HF_2^- in the samples (Figure 2), as noted previously,[17] results from F^- or XeF_2 attack on the solvent to produce HF which, in turn, reacts with F^- to form HF_2^-. The former and predominant reaction occurs by abstraction of H^+ from CH_3CN by F^-,[22] and by reaction of XeF_2 with CH_3CN.[23] The HF_2^- anion was not found to exchange with XeF_2 by either single selective inversion NMR spectroscopy (Figure 2) or by 2-D $^{19}F-^{19}F$ EXSY spectroscopy.[17]

Attempted Syntheses of the Cs^+ and $N(CH_3)_4^+$ Salts of XeF_3^-. In attempts to synthesize $[N(CH_3)_4][XeF_3]$, stoichiometric amounts of XeF_2 and $[N(CH_3)_4][F]$ were dissolved in CH_3CN solvent by briefly warming the mixture to room temperature, and in CHF_3 solvent at 0 °C (12 h) under autogenous pressure in a heavy-wall glass vessel. The Raman spectra of both samples were recorded at −160 °C under the frozen solvents and after solvent removal. Only bands arising from unreacted starting materials were observed, demonstrating that no XeF_3^- salts had formed based on calculated vibrational frequencies and Raman intensities of XeF_3^- (Table S1 in the Supporting Information). The inability to form a salt of the XeF_3^- anion in either CHF_3 or CH_3CN solvents parallels failed attempts to form $[N(CH_3)_4][F_3]$ from F_2 and $[N(CH_3)_4][F]$ in CH_3CN and CHF_3 solvents,[24] and was attributed to the high solvation energies of the fluoride ion in these polar solvents.

The syntheses of the Cs^+ and $N(CH_3)_4^+$ salts containing the XeF_3^- anion were also attempted in the absence of a solvent. Fusion of a 4-fold molar excess of XeF_2 with [Cs][F] resulted in no reaction up to 170 °C. When a 6-fold molar excess of XeF_2 with respect to $[N(CH_3)_4][F]$ was slowly heated to the melting point of XeF_2 (129 °C), rapid oxidative fluorination of the $N(CH_3)_4^+$ cation ensued along with detonation of the sample. The inability to form salts of the XeF_3^- anion prompted thermochemical and computational studies to investigate the formation of XeF_3^- in the solid state, gas phase, and in CH_3CN solution.

Thermochemistry. To account for failed attempts to prepare either the Cs^+ or the $N(CH_3)_4^+$ salt of the XeF_3^- anion, quantum-chemical calculations and established semiempirical methods[25−29] were used in conjunction with known thermodynamic quantities to estimate ΔH°_{rxn}, ΔS°_{rxn}, and ΔG°_{rxn} for eq 2 in the absence of a solvent. The standard enthalpies for the reactions were determined by analyzing their Born−Fajans−Haber cycles (eq 3). The enthalpy change for the gas-phase reaction (eq 4) corresponds to the negative of the fluoride ion affinity of XeF_2. A prior reported fluoride ion affinity value of 83.3 kJ mol^{-1} has been used.[1] The experimental

$$[M][F](s) + XeF_2(s) \rightarrow [M][XeF_3](s) \quad (2)$$

$$\Delta H^{\circ}_{rxn}([M][XeF_3], s) = H^{\circ}_{L}([M][F]) + \Delta H^{\circ}(XeF_2)_{sub} - FIA(XeF_2, g) - \Delta H^{\circ}_{L}([M][XeF_3]) \quad (3)$$

$$XeF_2(g) + F^-(g) \rightarrow XeF_3^-(g) \quad (4)$$

value for the enthalpy of sublimation ($\Delta H^{\circ}(XeF_2)_{sub}$) for XeF_2 (55.71 kJ mol^{-1}) was used.[30] The lattice enthalpies of [M][F] and $[M][XeF_3]$ were estimated by use of the volume-based method of Bartlett et al.[25,26] as generalized by Jenkins et al.[27,28] in eq 5, where R is the gas constant (8.314 J K^{-1} mol^{-1}), I is the ionicity of the salt, and the constants, α, β, and p, depend on the nature of the

$$\Delta H^{\circ}_{L} = 2I\left(\frac{\alpha}{\sqrt[3]{V_m}} + \beta\right) + pRT \quad (5)$$

salt. For the salts under investigation, which are singly charged and non-linear, the following values were used: $I = 1$, $\alpha = 117.3$ mm kJ mol^{-1}, $\beta = 51.9$ kJ mol^{-1}, and $p = 2$. In this formalism, ΔH°_{L} is the lattice enthalpy and is defined as the energy required to break the crystal lattice, and therefore has a positive value. The volume-based approach is particularly useful because the formula unit volume (V_m) of an unknown salt can be estimated with reasonable accuracy using several methods.[27,31,32] In the present case, $V_m([M][XeF_3] = V_m(XeF_2) + V_m([M][F])$, where $V_m(XeF_2) = 0.0622$ nm^3, $V_m([Cs][F]) = 0.0573$ nm^3, and $V_m([N(CH_3)_4][F]) = 0.1460$ nm^3, giving $V_m([Cs][XeF_3] = 0.1195$ nm^3 and $V_m([N(CH_3)_4][XeF_3] = 0.2082$ nm^3. The calculated lattice enthalpies are

$$\Delta H^{\circ}_{L}([Cs][F]) = 717 \text{ kJ mol}^{-1}$$

$$\Delta H^{\circ}_{L}([N(CH_3)_4][F]) = 554 \text{ J kJ mol}^{-1}$$

$$\Delta H^{\circ}_{L}([Cs][XeF_3]) = 585 \text{ kJ mol}^{-1}$$

$$\Delta H^{\circ}_{L}([N(CH_3)_4][XeF_3]) = 505 \text{ kJ mol}^{-1}$$

and net reaction enthalpies (eq 3) calculated for the reactions of [M][F] (M = $N(CH_3)_4$, Cs) with XeF_2 under standard conditions are

$$\Delta H^{\circ}_{rxn}([Cs][XeF_3], s) = 104 \text{ kJ mol}^{-1}$$

$$\Delta H^{\circ}_{rxn}([N(CH_3)_4][XeF_3], s) = 22 \text{ kJ mol}^{-1}$$

A method for estimating the absolute standard entropy of a salt from its unit volume has been reported by Jenkins and Glasser (eq 6) where $k = 1360$ J K^{-1} mol^{-1} nm^{-3}

(22) Christe, K. O.; Wilson, W. W. *J. Fluorine Chem.* **1990**, *46*, 339–342.
(23) Dukat, W. W.; Holloway, J. H.; Hope, E. G.; Townson, P. J. *J. Fluorine Chem.* **1993**, *62*, 293–296.
(24) Christe, K. O. *J. Fluorine Chem.* **1995**, *71*, 149–150.
(25) Bartlett, N.; Yeh, S.; Kourtakis, K.; Mallouk, T. *J. Fluorine Chem.* **1984**, *26*, 97–116.
(26) Shen, C.; Hagiwara, R.; Mallouk, T.; Bartlett, N. In *Inorganic Fluorine Chemistry, Toward the 21st Century*; Thrasher, J. S., Strauss, S. H., Eds.; ACS Symposium Series 555; American Chemical Society: Washington, DC, 1994; Chapter 2, pp 26−39.
(27) Jenkins, H. D. B.; Roobottom, H. K.; Passmore, J.; Glasser, L. *Inorg. Chem.* **1999**, *38*, 3609–3620.
(28) Jenkins, H. D. B.; Tudela, D.; Glasser, L. *Inorg. Chem.* **2002**, *41*, 2364–2367.
(29) Jenkins, H. D. B.; Glasser, L. *Inorg. Chem.* **2003**, *42*, 8702–8708.
(30) Osborne, D. W.; Flotow, H. E.; Malm, J. G. *J. Chem. Phys.* **1972**, *57*, 4670–4675.
(31) Jenkins, H. D. B.; Glasser, L.; Klapötke, T. M.; Crawford, M.-J.; Bhasin, K. K.; Lee, J.; Schrobilgen, G. J.; Sunderlin, L. S.; Liebman, J. F. *Inorg. Chem.* **2004**, *43*, 6238–6248.
(32) Elliott, H. St. A.; Lehmann, J. F.; Mercier, H. P. A.; Jenkins, H. D. B.; Schrobilgen, G. J. *Inorg. Chem.* DOI: 10.1021/ic101152x.

(formula unit)$^{-1}$ and $c = 15$ J mol^{-1} K^{-1}.[29]

$$S^\circ = kV_m + c \quad (6)$$

The standard entropies for the [M][F] and [M][XeF_3] are

$$S^\circ([Cs][F], s) = 92.9 \text{ J mol}^{-1} \text{ K}^{-1}$$

$$S^\circ([N(CH_3)_4][F], s) = 213.5 \text{ J mol}^{-1} \text{ K}^{-1}$$

$$S^\circ([Cs][XeF_3], s) = 177.5 \text{ J mol}^{-1} \text{ K}^{-1}$$

$$S^\circ([N(CH_3)_4][XeF_3], s) = 298.2 \text{ J mol}^{-1} \text{ K}^{-1}$$

The value determined for S°([Cs][F]) is in excellent agreement with the previously published value (92.8 J mol^{-1} K^{-1}).[33] When coupled with the experimental standard entropy of $XeF_{2(s)}$ (115.09 J mol^{-1} K^{-1}),[30] this method allows ΔS°_{rxn} (eq 7) and ΔG°_{rxn} (eq 8) to be calculated for the reactions of interest:

$$\Delta S^\circ_{rxn}([M][XeF_3], s) = S^\circ([M][XeF_3], s) - S^\circ(XeF_2, s) - S^\circ([M][F], s) \quad (7)$$

$$\Delta G^\circ_{rxn}([M][XeF_3], s) = \Delta H^\circ_{rxn}([M][XeF_3], s) - T\Delta S^\circ_{rxn}([M][XeF_3], s) \quad (8)$$

The ΔS°_{rxn} and ΔG°_{rxn} values obtained for these reactions are

$$\Delta S^\circ_{rxn}([Cs][XeF_3], s) = 30.5 \text{ J mol}^{-1} \text{ K}^{-1}$$

$$\Delta S^\circ_{rxn}([N(CH_3)_4][XeF_3], s) = 30.4 \text{ J mol}^{-1} \text{ K}^{-1}$$

$$\Delta G^\circ_{rxn}([Cs][XeF_3], s) = 114 \text{ kJ mol}^{-1}$$

$$\Delta G^\circ_{rxn}([N(CH_3)_4][XeF_3], s) = 31 \text{ kJ mol}^{-1}$$

The reaction enthalpies and Gibbs free energies are positive, indicating that both reactions are endothermic and nonspontaneous under standard conditions. The lattice enthalpy of [Cs][F] has also been derived from the published enthalpies of formation for this salt and gaseous Cs^+ and F^-,[33,34] giving a value of 756.0 kJ mol^{-1}. Use of this value gives a reaction enthalpy and Gibbs free energy that are even more unfavorable with respect to [Cs][XeF_3] formation:

$$\Delta H^\circ_{rxn}([Cs][XeF_3], s) = 143 \text{ kJ mol}^{-1}$$

$$\Delta G^\circ_{rxn}([Cs][XeF_3], s) = 152 \text{ kJ mol}^{-1}$$

As expected, the reaction employing the larger $N(CH_3)_4^+$ cation is far less endothermic and closer to spontaneity.

Computational Results. It was first suggested that the XeF_3^- anion would have an octahedral (meridional) AX_3E_3 (A = central atom, X = bonded electron pair, E = valence electron lone pair) valence shell electron pair repulsion (VSEPR) arrangement of bonded pairs and valence electron lone pairs (T-shaped geometry).[9] Although the *mer*-isomer of the XeF_3^- anion minimizes the lone pair-lone pair repulsions, there are no examples known in which three valence electron lone pairs are positioned at approximately 90° to one another. Because the XeF_3^- anion has thus far eluded solid-state characterization, computational chemistry was employed to help elucidate its structure in the gas phase as well as in CH_3CN solution through employment of a continuum solvent model. The thermodynamic properties of XeF_3^-, XeF_2, and F^- were also computed for comparison with the experimentally determined transition-state energy for the formation of the anion from XeF_2 and F^- in CH_3CN ($\Delta H^\ddagger = 65.5 \pm 8.4$ kJ mol^{-1}).

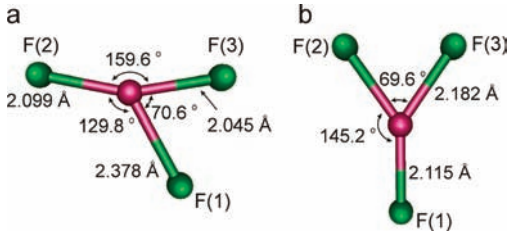

Figure 3. Calculated gas-phase geometries (PBE1PBE/aVTZ) of (a) the F_2Xe---F^- adduct (ground state, C_s symmetry), and (b) the XeF_3^- anion (transition state, C_{2v} symmetry).

To fully appreciate the complexity of this seemingly simple system, it is important to distinguish the two, discrete forms of the anion that have stationary points on the potential energy surface (PES), as computed in the present work and in previous studies:[1,14] a planar, distorted Y-shaped anion (C_s symmetry, Figure 3a) possessing two short Xe−F bonds and one long Xe−F bond (which is still within the sum of the van der Waals radii of xenon and fluorine, 3.63 Å[35]), and a planar, Y-shaped anion (C_{2v} symmetry, Figure 3b) possessing three similar Xe−F bond lengths. The former will be referred to as the F_2Xe---F^- adduct, while the latter will be referred to as the XeF_3^- anion. A third, T-shaped adduct of C_{2v} symmetry was also computed as a stationary point on the PES,[1,14] but it was found that a slight, symmetry-lowering distortion to C_s symmetry gave the lower energy, ground-state structure, which is, in fact, the *mer*-structure (albeit with one long Xe---F interaction). Finally, a Y-shaped anion (D_{3h}) was also computed as a diradical species, in accord with the structure predicted by molecular orbital (MO) theory,[14] but was found to be 59.8 to 110.0 kJ mol^{-1} higher in energy than the ground-state structure.

(a) Electronic Structures of the XeF_3^- and F_2Xe---F^- Anions. (i) In the Gas Phase. The optimized geometries of the XeF_3^-[14] and F_2Xe---F^-[1,14] anions have recently been reported; the results, along with the present work, are summarized in Table 1. In the former report, DFT calculations with the B3LYP functional indicated that the XeF_3^- anion (C_{2v}) is the energy-minimized structure (all frequencies real, Table S1 in the Supporting Information) when either an all-electron Maroulis basis set or an ECP basis set (SDB-cc-pVTZ) is used for xenon.[14] The F_2Xe---F^- adduct (C_{2v}) was higher in energy relative to the XeF_3^- anion by about 2.1−15.1 kJ mol^{-1},[14] and is a transition state (one imaginary frequency). However, the previous work[14] overlooked a lower-energy, ground-state conformation of the F_2Xe---F^- adduct possessing a lower symmetry (C_s), as found in a more

(33) Wagman, D. D.; Evans, W. H.; Parker, V. B.; Schumm, R. H.; Halow, I.; Bailey, S. M.; Churney, K. L.; Nuttall, R. L. *NBS Tables of Chemical Thermodynamic Properties*, Selected Values for Inorganic and C_1 and C_2 Organic Substances in SI Units. *J. Phys. Chem. Ref. Data* **1982**, *11* (Supplement 2), 367.
(34) ref 33, p 45.
(35) Bondi, A. *J. Phys. Chem.* **1964**, *68*, 441–451.

Table 1. Calculated[a] Gas-Phase and Solution-Phase (CH_3CN)[b] Geometries for the XeF_3^- and F_2Xe---F^- Anions

	XeF_3^-			F_2Xe---F^-			
	gas phase (C_{2v})	CH_3CN (C_{2v})	ref 14 (C_{2v})[c]	gas phase (C_s)	CH_3CN (C_s)	ref 14 (C_{2v})[c]	ref 1 (C_s)[d]
				Bond Lengths (Å)			
Xe−F(1)	2.084 (2.115)	2.026 (2.067)	2.161	2.567 (2.378)	3.035 (3.112)	2.681	2.510
Xe−F(2)	2.153 (2.182)	2.207 (2.230)	2.233	2.037 (2.099)	1.990 (2.009)	2.064	2.073
Xe−F(3)	2.153 (2.182)	2.207 (2.230)	2.233	1.970 (2.045)	1.983 (2.000)	2.064	2.002
				Bond Angles (deg)			
F(1) −Xe−F(2)	145.4 (145.2)	145.9 (146.0)	145.1	116.9 (129.8)	99.2 (99.2)	94.5	121.0
F(1) −Xe−F(3)	145.4 (145.2)	145.9 (146.0)	145.1	74.0 (70.6)	82.4 (82.6)	94.5	72.4
F(2) −Xe−F(3)	69.1 (69.6)	68.2 (68.1)	69.8	169.1 (159.6)	178.3 (178.2)	171.0	166.6

[a] CCSD/aug-cc-pVTZ(-PP) (PBE1PBE/aug-cc-pVTZ(-PP) values in parentheses). [b] Values were computed using the CPCM solvent model. [c] Values were computed using the B3LYP functional with an aug-cc-pVTZ basis set for F and a SDB-cc-pVTZ basis set for Xe. [d] CCSD(T)/aug-cc-pVTZ.

recent study (4.85 kJ mol^{-1} lower than the C_{2v} structure at the CCSD(T)/aVTZ level of theory).[1] Although the bond lengths for the adduct are incorrectly reported in the text, they are correct in the Supporting Information of ref 1. The latter bond lengths and angles are in good agreement with the bond lengths calculated for the F_2Xe---F^- adduct in the present study (Table 1). Furthermore, the existence of the XeF_3^- anion as a transition state was not explored.[1]

Calculations performed in the present work [DFT using the PBE1PBE functional, and CCSD; the basis sets used were aug-cc-pVTZ (F) and aug-cc-pVTZ-PP (Xe) and are hereafter referred to as "aVTZ" as in ref 1] were done without symmetry constraints, and reveal that the global-energy minimum of the anion is the F_2Xe---F^- adduct (C_s symmetry; Table 1, Figure 3a), in accord with the CCSD(T) results reported in the Supporting Information of ref 1. For the DFT structure, one of the Xe−F bonds is distinctly longer (2.378 Å) than the other two (2.045 and 2.099 Å), but well within the sum of the van der Waals radii for Xe and F.[35] The F−Xe−F fragment is slightly bent (159.6°) so that the structure can be viewed as XeF_2 perturbed by a fluoride ion, in agreement with the previous work.[1] Although the qualitative agreement with the geometries optimized at the DFT and CCSD levels is good, the geometric parameters (Table 1) show that the PBE1PBE functional predicts a structure in which F(1) is more strongly bound to the XeF_2 fragment, whereas the coupled-cluster method predicts a significantly longer Xe−F(1) bond length (2.561 Å) and a more open F(2)−Xe−F(3) bond angle (169.1°).

To elucidate the structure of the transition state, a scan involving the stepwise reduction in the long Xe−F bond length of the F_2Xe---F^- adduct was computed. In both cases (PBE1PBE and CCSD), the transition-state structure was that of the Y-shaped XeF_3^- anion (Figure 3b). The structures thus obtained were further optimized as transition states at their respective levels of theory (Table 1). Calculations were also performed to determine if the T-shaped, C_{2v}-symmetric transition state was a potential competing transition state. The C_{2v}-symmetric transition state was 14.6 (PBE1PBE) and 16.7 (CCSD) kJ mol^{-1} higher in energy than the Y-shaped XeF_3^- anion, indicating that the latter is the more favored transition state. Thermodynamic calculations for the intermolecular exchange between XeF_2 and F^- were also reinvestigated in the present work (see Computational Assessment of Intermolecular Exchange).

The transition state (XeF_3^-) is more strongly covalently bound than the ground-state F_2Xe---F^- adduct. When DFT methods are used, the XeF_3^- anion possesses three similar Xe−F bond lengths (2.115 Å and 2.182 Å (×2)). The two large (145.2°) angles and one small (69.6°) angle allow for the retention of the lone-pair torus around the xenon atom, as shown by ELF analyses (see Electron Localization Function (ELF) Analyses). The structure computed at the CCSD/aVTZ level of theory was found to possess similar geometric parameters to that of the DFT structure (Table 1). It is unclear why the XeF_3^- anion was computed to be an energy minimum in the previous study[14] since the structure remains a transition state even when the calculations are performed using the same basis set-density functional combination as employed in the prior work.

(ii) In CH_3CN Solution. Because the enthalpy of activation of F^- ion exchange with XeF_2 in CH_3CN solvent was found to be in good agreement with the experimental findings (see Computational Assessment of Intermolecular Exchange between F^- and XeF_2), the structures for F_2Xe---F^- and XeF_3^- were also determined in CH_3CN using the CPCM model[36] (Table 1). For the F_2Xe---F^- adduct, the bond between XeF_2 and F^- loses some of its covalent character. The optimized structure contains a near-linear XeF_2 fragment (PBE1PBE, 178.2°; CCSD, 178.3°) with a long Xe−F bond equal to 3.112 Å (PBE1PBE) and 3.035 Å (CCSD) that is still significantly less than the sum of the Xe and F van der Waals radii. Unlike the gas-phase structures, the geometric parameters in CH_3CN solution do not change significantly between the PBE1PBE and CCSD levels (Table 1), and show that the interaction between XeF_2 and F^- is primarily electrostatic in nature, precluding the observation of an F_2Xe---F^- adduct by ^{19}F NMR spectroscopy in this solvent or by low-temperature Raman spectroscopy in frozen CH_3CN solution. In contrast to the adduct, the geometry for the XeF_3^- anion modeled in CH_3CN solution remains essentially unchanged from that determined in the gas phase (Table 1).

(b) Computational Assessment of Intermolecular Exchange between F^- and XeF_2. (i) In the Gas Phase. In light of the ^{19}F NMR spectroscopic study (see Intermolecular Exchange Between F^- and XeF_2), the reaction between XeF_2 and F^- was modeled by a series of computational scans with optimizations of the stationary points (PBE1PBE and CCSD) to (1) establish the exchange pathway, and to (2) determine how well the calculated thermodynamics agree with the experimental ^{19}F NMR spectroscopic results. Although

(36) Barone, V.; Cossi, M. *J. Phys. Chem. A* **1998**, *102*, 1995–2001.

Table 2. Gas-Phase and Solution-Phase (CH_3CN)[a] Natural Bond Orbital (NBO) Analyses and Natural Population Analysis (NPA) Charges for the XeF_3^- and F_2Xe---F^- Anions[b]

	XeF_3^-		F_2Xe---F^-	
	gas phase	solution phase	gas phase	solution phase
		Natural Charges		
Xe	1.227 (1.097)	1.242 (1.161)	1.292 (1.130)	1.289 (1.260)
F(1)	−0.720 (−0.684)	−0.661 (−0.654)	−0.956 (−0.817)	−0.996 (−0.995)
F(2)	−0.753 (−0.707)	−0.791 (−0.754)	−0.699 (−0.681)	−0.650 (−0.636)
F(3)	−0.753 (−0.707)	−0.791 (−0.754)	−0.636 (−0.633)	−0.642 (−0.629)
		Bond Orders		
Xe−F(1)	0.219 (0.255)	0.287 (0.260)	0.020 (0.155)	0.007 (0.011)
Xe−F(2)	0.167 (0.229)	0.169 (0.173)	0.248 (0.259)	0.306 (0.297)
Xe−F(3)	0.167 (0.229)	0.169 (0.173)	0.292 (0.293)	0.310 (0.301)

[a] Values were computed using the CPCM solvent model. [b] CCSD/aVTZ//CCSD/aVTZ and PBE1PBE/aVTZ//PBE1PBE/aVTZ where the latter are given in parentheses.

the energy profile for the direct fluoride ion loss from the XeF_3^- anion was recently calculated at the DFT level,[14] failure to obtain the correct ground-state and transition-state structures (see Electronic Structures of the XeF_3^- and F_2Xe---F^- Anions) led to an erroneous interpretation of the exchange thermodynamics.

The stepwise elongation of the long Xe−F bond of the F_2Xe---F^- adduct (i.e., the FIA) within the C_s symmetry constraint led to a smooth increase in the total energy of the system with an asymptotic (optimized) value of 97.1 kJ mol^{-1} at the PBE1PBE/aVTZ level of theory (115.3 kJ mol^{-1} at the CCSD/aVTZ level of theory). The PBE1PBE energy is in good agreement with the gas-phase fluoride ion affinities determined in previous experimental (81.2 ± 5.9 kJ mol^{-1})[14] and theoretical (96.7[14] and 83.3[1] kJ mol^{-1}) studies. Conversely, the stepwise shortening of the long Xe−F bond of the F_2Xe---F^- adduct (i.e., the enthalpy of activation) resulted in the XeF_3^- anion as the transition state. The enthalpy change in going from the ground state to the transition state was small (PBE1PBE, $\Delta H^{\ddagger} = 1.3$ kJ mol^{-1}; CCSD, $\Delta H^{\ddagger} = 13.4$ kJ mol^{-1}). Although the gas-phase results indicate that the FIA of XeF_2 is sufficient to form the F_2Xe---F^- adduct in the solid state, salts of the XeF_3^- anion could not be formed in solution or in the solid state by reaction of XeF_2 with [Cs][F] or $[N(CH_3)_4][F]$. Furthermore, the energy barrier to fluoride ion exchange between XeF_2 and F^- (i.e., the formation of the XeF_3^- anion) is very small in contrast with the experimental findings. Therefore, in an attempt to reconcile the experimental and computational findings, the thermodynamics of the XeF_2/F^- exchange were modeled in CH_3CN.

(ii) In CH_3CN Solution. In marked contrast with the gas-phase results, the stepwise elongation of the long Xe−F bond of the F_2Xe---F^- adduct (i.e., the FIA) yielded a much smaller increase in the enthalpy (PBE1PBE, 5.0 kJ mol^{-1}; CCSD, 7.1 kJ mol^{-1}). The enthalpy of formation from XeF_2 and F^- suggests that XeF_2 possesses little to no affinity for the fluoride ion in CH_3CN solution. Because the enthalpy of formation is small for the F_2Xe---F^- adduct, the enthalpy for the formation of XeF_3^- (i.e., the enthalpy of activation) could be determined relative to free XeF_2 and F^-, and gave energy barriers for the fluoride ion exchange reaction that were much higher than those in the gas phase: 24.7 (PBE1PBE) and 50.2 kJ mol^{-1} (CCSD). While the value obtained using the PBE1PBE functional was underestimated, the value obtained using the CCSD method fell within the range of those experimentally determined for the fluoride ion exchange (65.5 ± 8.4 kJ mol^{-1}). Taken as a whole, the calculations confirm that the direct reaction between XeF_2 and F^- in solution leads to fluoride ion exchange via a transition state corresponding to the Y-shaped XeF_3^- anion.

Finally, to assess the validity of averaging the two activation enthalpies obtained by ^{19}F NMR spectroscopy (i.e., that the two energies do not correspond to two different transition states existing at two different concentrations), other possible transition states on the PES were explored. Both XeF_4^{2-} and $XeF_3^- \cdot XeF_2$ were assessed using the CH_3CN solvent model at both the PBE1PBE/aVTZ and MP2/aVTZ levels of theory, but dissociated to XeF_3^- and F^- and to XeF_3^- and XeF_2, respectively. These calculations lend further support to the view that the XeF_3^- anion is the only viable transition state in the exchange between XeF_2 and F^-.

(c) Natural Bond Orbital (NBO) Analyses. The results from the NBO analyses conducted for XeF_3^- and F_2Xe---F^- are collected in Table 2. The calculated natural population analysis (NPA) charges for the F_2Xe---F^- adduct (from PBE1PBE and CCSD geometries, respectively) show that the combined charge of the XeF_2 fragment is near zero (−0.18/−0.04), and that the negative charge is distributed unevenly among the three fluorine atoms, with F(1) carrying most of the charge (−0.82/−0.96). The Lewis-like depiction that approximates the total electron density given by the NBO analysis is one in which the bonding in the F_2Xe---F^- adduct has two major contributions; (1) bonding Xe−F interactions within the F(2)−Xe−F(3) fragment (Xe−F bond orders of 0.259/0.248 and 0.293/0.292) and (2) a weak covalent interaction between neutral XeF_2 and F^- (Xe−F(1) bond order of 0.155/0.020), which is calculated to be much stronger using the PBE1PBE method. Using the solvent model, the bond orders for the PBE1PBE and CCSD structures become more similar, with slightly stronger Xe−F(2)/F(3) interactions (0.297/0.306 and 0.301/0.310, respectively) and a much weaker Xe−F(1) interaction (0.011/0.007).

In contrast to the F_2Xe---F^- adduct, the XeF_3^- anion is a covalently bound Y-shaped anion (C_{2v}), with all the fluorine atoms having similar charges (PBE1PBE: −0.67, −0.71, and −0.71; CCSD: −0.72, −0.75 and −0.75), and also possessing similar bond orders (PBE1PBE: 0.262, 0.204, and 0.204; CCSD: 0.219, 0.167, and 0.167). These values do not change substantially when modeled in CH_3CN solution (Table 2).

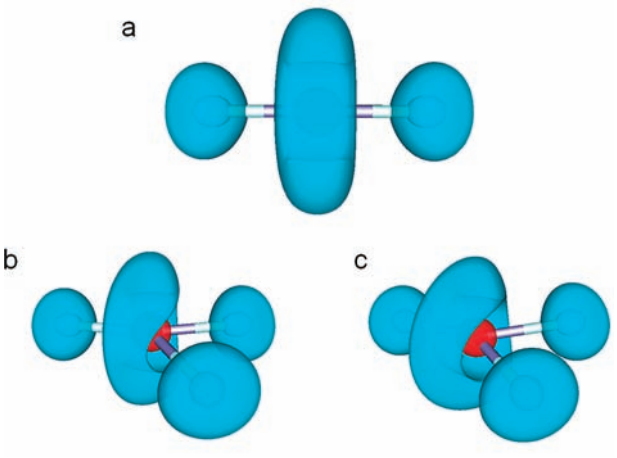

Figure 4. Electron localization function isosurfaces (contour level 0.7) of (a) XeF_2, (b) the $F_2Xe{---}F^-$ adduct, and (c) the XeF_3^- anion (calculated at the PBE1PBE/aVTZ level of theory). Color scheme: blue, lone-pair (monosynaptic) basin; red, core basin.

(d) Electron Localization Function (ELF) Analyses. The use of ELF for inorganic systems containing xenon has proven useful for qualitative analysis.[37,38] It is also well-known that while ELF analyses can be instructive, there is no direct physical interpretation for an ELF basin or its population.

The linear structure of XeF_2, and its calculated ELF isosurface (performed on the PBE1PBE/aVTZ-optimized geometry) shows a torus composed of the three lone pairs around xenon (Figure 4a). Addition of a fluoride ion results in a distortion of the lone pair torus upon addition of another bonding pair of electrons and an increase in electron−electron repulsion. This repulsion is reduced by lowering the symmetry from C_{2v} to C_s, allowing the fluoride ion to avoid a "head-on" interaction with the electron lone-pair torus (Figure 4b), and keeping the fluoride distance longer than a typical covalent Xe−F bond (Table 1). In contrast to the $F_2Xe{---}F^-$ adduct, the XeF_3^- anion shows strong covalent bonding for all three fluorine atoms. Where VSEPR would predict a *mer*-arrangement (based on an octahedral arrangement of bond pairs and lone pairs), computations show a highly distorted, planar Y-shaped geometry with C_{2v} symmetry. The ELF analysis (Figure 4c) indicates that the distortion arises from retention of the torus about the xenon atom. In contrast with the $F_2Xe{---}F^-$ adduct, the torus is not as strongly distorted toward the F(1) atom, and away from the F(2) and F(3) atoms. It is energetically more favorable to have a F−Xe−F angle of 69° than it is to have three xenon lone pairs at ca. 90° to one another in a T-shaped (meridional) structure.

Conclusions

The standard enthalpy of formation for the intermolecular ^{19}F exchange between XeF_2 and $[N(CH_3)_4][F]$ in CH_3CN solvent was measured by single selective inversion NMR spectroscopy and determined to be 65.5 ± 8.4 kJ mol^{-1}. The inability to synthesize salts containing the XeF_3^- anion in the present work is attributed to the low fluoride ion affinity of XeF_2. The calculated energy-minimized geometries (PBE1PBE and CCSD) of the $F_2Xe{---}F^-$ and XeF_3^- anions show distorted Y-shaped (adduct) and Y-shaped (anion) structures, respectively. Computed enthalpies using the CH_3CN solvent model demonstrated that XeF_2 has no affinity for the fluoride ion in solution, and gave activation enthalpies (CCSD) that agreed well with the experimentally determined activation enthalpy.

Experimental Section

Materials and Synthetic Techniques. Fluoroform, CHF_3 (Canadian Liquid Air, 98%) was condensed from a metal vacuum line. Prior to introduction into the vacuum manifold, CHF_3 gas was passed through a copper coil cooled to −78 °C in solid dry ice. Preparation of all other starting materials and standard techniques were conducted as previously described,[17] unless otherwise specified.

Attempted Syntheses of Salts Containing the XeF_3^- Anion. Inside a drybox, $[N(CH_3)_4][F]$ (0.01620 g, 0.01739 mmol) and XeF_2 (0.02960 g, 0.01749 mmol) were loaded into a glass thick-wall h-shaped reaction vessel (9-mm o.d., 2.5-mm i.d.). The reaction vessel was attached to a stainless steel vacuum line and anhydrous CHF_3 was condensed into the vessel. Once the reaction vessel was flame-sealed it was placed in a dewar flask containing a 95% ethanol/liquid nitrogen slush at ca. −110 °C. The reaction mixture was then agitated over a period of 30 min while warming to 0 °C and allowed to stand for 12 h. The sample was mixed again, and a Raman spectrum was recorded at −160 °C directly on the thick-walled glass reaction vessel containing the solid sample. The CHF_3 was distilled into one arm of the reaction vessel and was flame-sealed off. A white, crystalline powder was obtained, and Raman spectra were recorded at −155 °C directly on the sealed off portion of the thick-wall glass reaction vessel containing the solid sample.

Equimolar amounts of $[N(CH_3)_4][F]$ (0.01620 g, 0.1739 mmol) and XeF_2 (0.02960 g, 0.1749 mmol) were also loaded into a $^1/_4$-in. glass tube fused to a 5-mm o.d. thick-wall glass NMR tube, inside a drybox. The reaction vessel was attached to a stainless steel vacuum line and anhydrous CHF_3 was condensed into the vessel at −196 °C to a height of ca. 5 cm, and the sample tube and contents were cooled to −196 °C and flame-sealed under vacuum. The reaction vessel was warmed in stages up to room temperature and maintained at 0 °C for 12 h. After cooling to −78 °C, a white, crystalline powder precipitated, and the Raman spectra of the solid under frozen solvent was recorded at −160 °C (directly on the upper and lower regions of the sealed off portion of the thick-wall glass reaction vessel containing the solid sample), and confirmed that no reaction had occurred.

Equimolar amounts of $[N(CH_3)_4][F]$ (0.01474 g, 0.1582 mmol) and XeF_2 (0.02394 g, 0.1414 mmol) were added to a 4-mm o.d. FEP reaction vessel. Dry CH_3CN solvent was then added to the sample and reacted for ca. 1 h at −30 °C. The solvent was removed under vacuum at −30 °C and a Raman spectrum was recorded at −160 °C on the non-volatile residue, confirming that no reaction had occurred.

Cesium fluoride (0.08105 g, 0.5336 mmol) and XeF_2 (0.38827 g, 2.294 mmol) were loaded into a 4-mm o.d. FEP tube. The tube was then heat sealed under ca. 0.5 atm N_2, and then immersed in an oil bath and heated to 170 °C. A Raman spectrum recorded at −155 °C confirmed that no reaction had occurred. A sample of $[N(CH_3)_4][F]$ (0.02076 g, 0.0223 mol) and XeF_2 (0.23772 g, 1.404 mmol) was similarly prepared. The sample was immersed in an oil bath and detonated violently at the melting point of XeF_2 (129 °C).

Nuclear Magnetic Resonance Spectroscopy. Single selective inversion experiments were conducted as previously described and the full observed relaxation,[21] under the combined influence of spin−lattice relaxation and chemical exchange, was analyzed using the CIFIT program.[39] Equimolar samples of XeF_2 and

(37) Mercier, H. P. A.; Moran, M. D.; Sanders, J. C. P.; Schrobilgen, G. J.; Suontamo, R. J. *Inorg. Chem.* **2005**, *44*, 49–60.
(38) Brock, D. S.; Casalis de Pury, J. J.; Mercier, H. P. A.; Schrobilgen, G. J.; Silvi, B. *Inorg. Chem.* **2010**, *49*, 6673–6689.
(39) Bain, A. D.; Duns, G. J.; Rathgeb, F.; Vanderkloet, J. *J. Phys. Chem.* **1995**, *99*, 17338–17343.

$[N(CH_3)_4][F]$ were prepared in CH_3CN solvent with concentrations of 0.18 and 0.36 M, as described previously.[17]

Fluorine-19 NMR spectra were referenced to external $CFCl_3$ at 30 °C. The NMR probe was cooled using a nitrogen flow and variable temperature controller (BV-T 2000). All spectra in this study were recorded unlocked (field drift < 0.1 Hz h^{-1}). The NMR spectra were recorded on a Bruker DRX-500 spectrometer and acquired at 470.560 MHz in 64 K memories over a 14.86 kHz spectral width corresponding to an acquisition time of 0.23 s and a data point resolution of 2.18 Hz/point.

Raman Spectroscopy. Low-temperature (−155 to −165 °C) Raman spectra were recorded on a Bruker RFS 100 FT Raman spectrometer using 1064-nm excitation as previously described.[40] Spectra were recorded in glass or $^1/_4$-in. FEP sample tubes using a laser power of 200 mW and a total of 300 scans.

Computational Methods. Molecular geometries were optimized with CCSD and DFT (using the PBE1PBE exchange-correlation functional) with aug-cc-pVTZ (F) and aug-cc-pVTZ-PP (Xe) basis sets (basis sets obtained from https://bse.pnl.gov/bse/portal). The nature of all stationary points found was assessed by performing frequency analyses. Calculations involving solvent effects were performed using the CPCM model[36] and employing the default parameters for CH_3CN. Natural atomic orbital and natural bond orbital analyses were conducted using the NBO 5.0 code;[41] electron localization function analyses were performed with the program package TopMod.[42] Visualizations of molecular structures and ELF isosurfaces were done with the gOpenMol program.[43,44] Quantum-chemical calculations were carried out using the program Gaussian 09[45] for geometry optimizations, vibrational frequencies, and their intensities and the program Gaussian 03[46] for NBO analysis.

Acknowledgment. This work is dedicated to the memory of Dr. Donald W. Hughes (1949-2010). We thank the Natural Sciences and Engineering Research Council of Canada for the award of a postgraduate scholarship (N.V.) and for support in the form of a Discovery Grant (G.J.S.). We also thank the Academy of Finland (H.M.T.) for financial support.

Supporting Information Available: Calculated gas-phase frequencies (cm^{-1}) and relative Raman intensities for the XeF_3^- and $F_2Xe{-}{-}{-}F^-$ anions (Table S1); complete references 45 and 46. This material is available free of charge via the Internet at http://pubs.acs.org.

(40) Gerken, M.; Dixon, D. A.; Schrobilgen, G. J. *Inorg. Chem.* **2000**, *39*, 4244–4255.

(41) Glendening, E. D.; Badenhoop, J. K.; Reed, A. E.; Carpenter, J. E.; Bohmann, J. A.; Morales, C. M.; Weinhold, F. *NBO*, 5.0; Theoretical Chemistry Institute, University of Wisconsin: Madison, WI, 2001.

(42) Noury, S.; Krokidis, X.; Fuster, F.; Silvi, B. *TopMod package*; University of Paris VI: Paris, 1998.

(43) Laaksonen, L. *J. Mol. Graph.* **1992**, *10*, 33–34.

(44) Bergman, D. L.; Laaksonen, L.; Laaksonen, A. *J. Mol. Graph. Model.* **1997**, *15*, 301–306.

(45) Frisch, M. J. et al. *Gaussian 09* (Revision A.02); Gaussian, Inc.: Wallingford, CT, 2009.

(46) Frisch, M. J.; et al. *Gaussian 03* (Revision D.01); Gaussian, Inc.: Wallingford, CT, 2004.